Optical Properties of the Hall D Fibre Calorimeter

Kiri Nichol*

Department of Physics and Astronomy, University of British Columbia

6224 Agricultural Road, Vancouver,

British Columbia, Canada, V6T 1Z1

(Dated: September 11, 2003)

Abstract

The barrel calorimeter (BCAL) designed for Hall D at Jefferson Labs utilizes scintillating fibres to improve resolution. Examining the optical properties of these fibres with analytical and computational methods suggests several possible improvements to the current calorimeter design. Double-clad fibres are shown to have no optical advantage over single-clad fibres.

PACS numbers:

*Electronic address: kiri@physics.ubc.ca

I. TABLE OF CONTENTS

II. INTRODUCTION

The GlueX / Hall D project at Jefferson Labs in Newport News, Virginia, will study the fundamental prediction of quantum chromodynamics (QCD) by examining the origins of quark confinement through detailed measurements of exotic hybrid mesons. QCD supposes that quarks interact through a "colour" charge ("red", "green" and "blue") carried by gluons. Quarks form "colourless objects", either through a quark-antiquark pairing or through the coupling of three quarks, one red, one green and one blue. That quarks are bound in triplets and pairs and are never found alone is a phenomenon is known as "confinement" [1].

The Hall D experiment will focus on photo-produced mesons and the study of new, exotic forms of matter. Because all the products of a decay must be observed to reconstruct the parent particles, the Hall D detector utilizes a hermetic design based on a central solenoidal cryo-magnet. A crucial component of this detector is the Barrel Calorimeter (BCAL), which will measure particles emitted radially in a direction normal to the incident beam [2]. The calorimeter designed for the GlueX experiment will primarily detect photons produced through the decay of π^0 and η particles which are, in turn, emitted by mesons or excited baryons [2].

The calorimeter consists of alternating layers of lead and scintillating fibres, fixed together with optical glue. The fibre-based design permits higher resolution measurements than a sheet calorimeter design while continuing to be relatively cheap. The fibres are made from fast plastic scintillator material (Pol.hi.tech 0046-100) which allows integrated signal times to be kept below 100 ns. Two kinds of fibre are presently available - a double-clad model in which a core of 1.59 index plastic is surrounded by thin layers of 1.49 and 1.42 index plastic, and a single-clad model in which there is one layer of 1.49 index cladding. In the single-clad fibre, the radius of the core is 0.0485 mm and the width of the cladding is 0.0015 mm.

Because it is important to extract a strong, sharp signal from the fibres, improvements to the effectiveness of the BCAL may be made by examining the optical behaviour of the fibres.

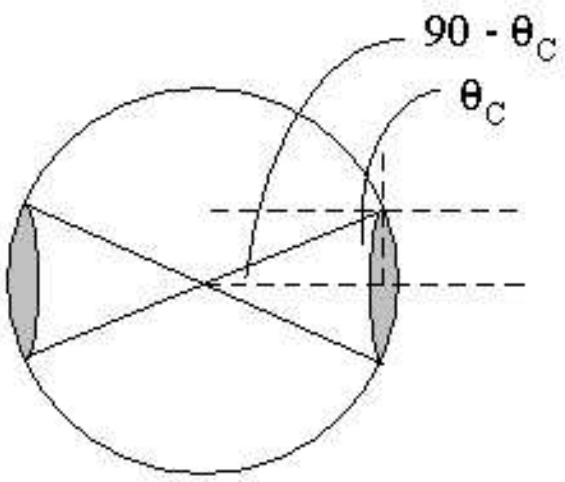

FIG. 1: Rays passing through the shaded area will undergo TIR.

III. THEORY

The fraction of light transmitted from an isotropic point source at the centre of a fibre can be determined analytically in the following manner: if a sphere is drawn around a point source, the fraction of rays emitted at an angle such that the photons will undergo total internal reflection (TIR) for the length of the fibre will be given by the ratio of the area of the shaded surface to the total area of the sphere as shown in Figure 1. The critical angle, θ_c, is defined by Snell's Law (Equation 1) where n_2 is the refractive index of the cladding (or the exterior environment, whichever is lower) and n_1 is the index of the core material. The area of the shaded segment is given by Equation 2.

$$\sin\theta_c = \frac{n_2}{n_1} \tag{1}$$

$$\begin{aligned} Area &= \tfrac{2}{3}R^3 \int_0^{2\pi}\int_0^{\pi/2-\theta_c} \sin(\theta)d\theta d\phi \\ &= 1-\sin\theta_c \\ &= \tfrac{n_1-n_2}{n_1} \end{aligned} \tag{2}$$

Equation 2 reproduces the trapping efficiency values reported in the Kuraray manual [4]. Note that Equation 2 yields overall transmission in both directions up and down the fibre are thus gives twice the magnitude of the trapping efficiencies in the Kuraray documentation, in which transmission only occurs in one direction.

The simplicity of Equation 2 results from the observation that the transmission efficiency of the fibres is independent of the number of layers of cladding. Instead, the fraction of the rays reaching the end of the fibre depends only on the refractive index of the core material and on the lowest index material from among the cladding or the surroundings. Thus, there is no apparent optical advantage to be gained by using multi-clad fibres in the Hall D Barrel Calorimeter.

IV. TIMING INFORMATION FROM WAVEFORM SHAPE

Because rays passing into the cladding will travel more quickly than rays undergoing TIR in the core material, the characteristic signal detected by the PMTs at the ends of the fibre spreads out in time in a manner which is dependent on the distance of the detector from the source. This property could potentially be used to determine how far down the fibre an event occurred.

To determine if the structure of the waveform detected by the PMT could be used to solve for the event location, a model was generated in Maple (Appendix 1). In this scenario, photons are generated at the centre of the fibre and proceed down the length of the system, escaping, reflecting or refracting as given by the electromagnetic equations in Griffiths [3]. The time required for a photon to reach the end of the fibre is evaluated as function of the emission angle (Ω in Figure 2. If the probability of reflection at the cladding/core boundary is 95%, 5% of the rays originating at the centre of the fibre will pass into the cladding before returning to the centre of the core, while the remaining 95% reflect at the core-cladding boundary. This crude approximation begins to fail at higher reflection coeffecients and does not yield any information about the binomial nature of the distribution of the transmission times.

At the core-cladding boundary, there is a jump in the transmission time (Figure 3). This jump produces a characteristic drop-off in the number of counts received as a function of time (Figure 4). Furthermore, adjusting the width of the cladding and core changes the the shape of the characteristic bin-time curve. In Figure 5, the cladding and the core have the same radius and the drop-off apparent in Figure 4 has been eliminated.

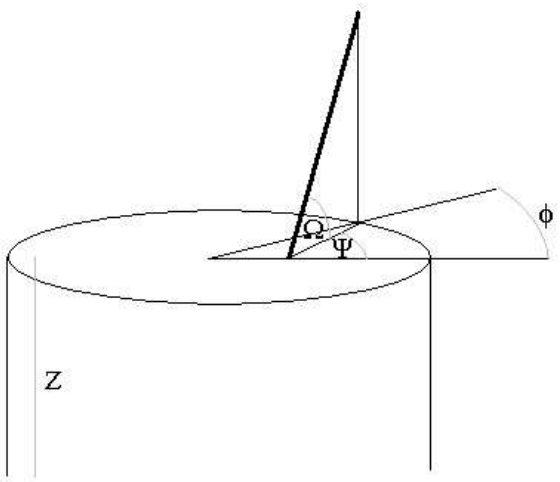

FIG. 2: Simulation geometry. Random values are assigned to $\sin\Omega$, Ψ, R to model isentropic point sources at different radii. Random values can also be assigned to Z to approximate the behaviour of real scintillating fibres.

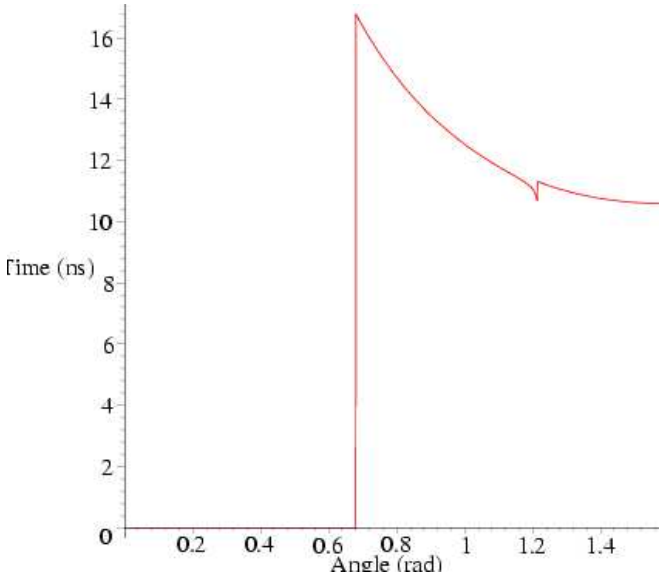

FIG. 3: Transmission time (ns) as a function of angle. The angle, θ is measured as in Figure 1. The transmission time for a ray emitted from the centre of the fibre at a given angle is evaluated for the most likely path, as given by the probabilities of reflection and transmission at the core-cladding boundary.

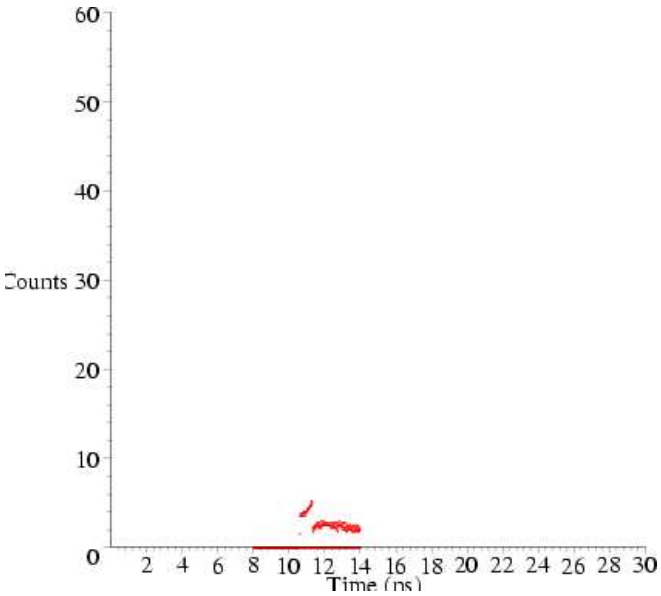

FIG. 4: Theoretical number of counts received as a function of transmission time (ns). The fibre is single-clad (n2 = 1.49) and lies in air. The times recorded are for the most probable path and are based the model described in Appendix 1.

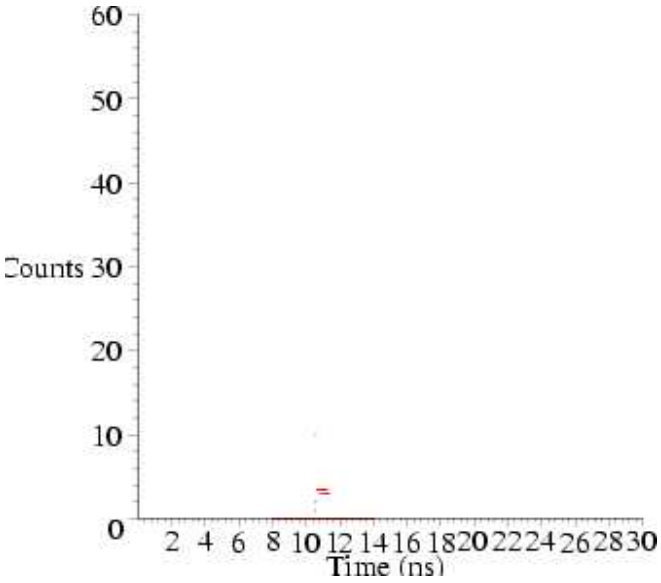

FIG. 5: Theoretical number of counts received as a function of transmission time (ns). The fibre is single-clad (n2 = 1.49) and lies in air, however the radius of the cladding and the radius of the core are both 0.05 mm. The times recorded are for the most probable path and are based the model described in Appendix 1 .

TABLE I: Transmission in Fibres

Randomized Initial Conditions	Cladding Index	External Index	% Transmission (Theory)	% Transmission (Model)
Ψ, $\sin(\Omega)$	1.49	1.00	37.1	37.6 (1.4)
Ψ, R, $\sin(\Omega)$	1.49	1.00	37.1	58.1 (1.4)
Ψ, R, $\sin(\Omega)$	1.42	1.00	37.1	57.0 (1.4)
Ψ, R, $\sin(\Omega)$	1.49	1.56	6.3	12.1 (1.4)
Ψ, R, $\sin(\Omega)$	1.42	1.56	10.7	21.3 (1.4)

V. MONTE-CARLO SIMULATION

The transmission efficiency for the case in which the rays do not originate from the the centre of the fibre cannot be solved analytically. In order to determine the exact transmission efficiency, ray-tracing software must be implemented to solve cases in which the source does not originate at the centre ($R = 0$) of the fibre. The ray-tracing program written to solve this problem places isotropic point sources at random radii. The initial ray is generated using random values of $\sin\Omega$ and Ψ, as defined in Figure 2.

VI. RESULTS

The waveform shape predicted by the analysis in Maple is significantly spread out when the initial radius is randomized. This spread occurs to such an extent that the shape of the signal is no longer useful for determining the location at which the photons were generated. The resolution of the PMTs is, under normal conditions, 0.5 ns and the shape of the waveform is only just resolvable at this scale. In addition, the source signal will be generated over a length of a few centimetres in the fibre and this blurs the characteristic drop in counts over a range of bins - in Figure 6 this drop occurs at about 13 ns. However, Figure 7 is generated with random values of Z chosen over a 4cm range and the characteristic drop-off becomes indistinct.

Table I displays the analytical values calculated from Equation 2. The first entry, in which Ψ and $\sin\Omega$ were assigned random values and the radius at the origin of the ray was zero, reproduces the result predicted analytically.

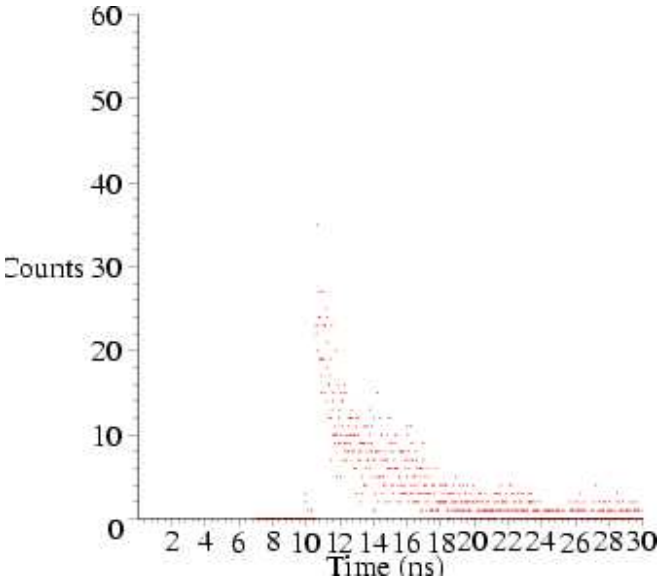

FIG. 6: Monte-Carlo simulation of counts received as a function of transmission time (ns). The fibre is single-clad ($n_2 = 1.49$) and lies in air. R, $\sin\Omega$ and Psi are given random values.

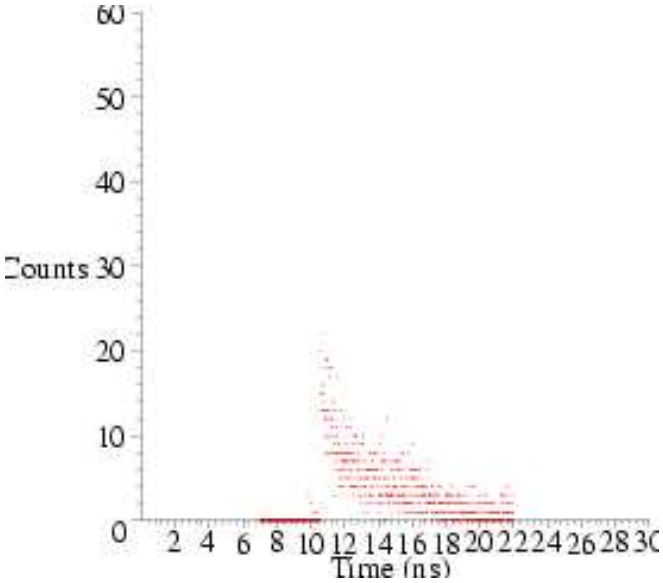

FIG. 7: Monte-Carlo simulation of counts received as a function of transmission time (ns). The fibre is single-clad ($n_2 = 1.49$) and lies in air. R, Z, $\sin\Omega$ and Ψ are given random values. Data collection was truncated after 22 ns.

Both the 1.49-index clad fibre and the 1.42-index clad fibre yield equal transmission efficiences in air. This is consistent with the expectation that transmission depends only on the core index and lower of the two indices in the cladding and the surroundings. The

transmission efficiency in the simulated fibres is higher than the transmission efficiency predicted analytically by Equation 2 due to geometric effects of placing the source outside the centre of the fibre.

VII. CONCLUSION

The behavior of light produced in scintillating fibres was examined using analytical and Monte-Carlo techniques. Transmission in the fibre was found to be independent of any layering in the cladding. In the case where the index of refraction of the cladding was lower than the index of the outside material (glue), the fraction of light transmitted to the end of the fibre is dependent only on the refractive indices of the core material and the exterior cladding material. In the case where the index of refraction of the cladding was higher than the index of the outside material (air or glue), the fraction of light transmitted to the end of the fibre is dependent only on the refractive indices of the core material and the external environment. Because of this, double-clad fibres are unneccessary and an extra expense - a single clad fibre in which the cladding has the lowest possible refractive index would be the most desirable for use in the Hall D barrel calorimeter.

Transmission of optical signals in the BCAL dectector would be also improved if the fibres could be mounted in air or a low-index glue instead of high-index optical adhesive.

VIII. ACKNOWLEDGMENTS

The Monte-Carlo simulation software used in this investigation was written and implemented with Ryan Ziegler. I would also like to thank my supervisors, Edward Brash, George Lolos and Zisis Papandreou.

IX. BIBLIOGRAPHY

[1] L. Snook. Hybrid Photomultiplier Tubes for Hall D/Jefferson Lab. Aug 2001. http://www.phys.uregina.ca/halld/reports/2001/HPMT/

[2] Jefferson Lab. "The Science Driving the 12 GeV Upgrade of CEBAF". 2001.

[3] D. J. Griffiths. *Introduction to Electrodynamics*. Prentice-Hall. 1981.

[4] Kuraray Co. Ltd. "Kuraray's Scintillation Materials". Metlife Bldg., 200 Park Avenue, New York.

X. APPENDIX 1

The Maple worksheet attached here is available in home/nichol/maple_ray-tracing/histogram_rays4.mws.